

Opportunistic search for continuous gravitational waves from compact objects in long-period binaries

AVNEET SINGH^{1,2} AND MARIA ALESSANDRA PAPA^{1,2,3}

¹*Max-Planck-Institut für Gravitationsphysik (Albert-Einstein-Institut), D-30167 Hannover, Germany*

²*Leibniz Universität Hannover, 30167 Hannover, Germany*

³*Department of Physics, University of Wisconsin, Milwaukee, WI 53201, USA*

ABSTRACT

Most all-sky searches for continuous gravitational waves assume the source to be isolated. In this paper, we allow for an unknown companion object in a long-period orbit and opportunistically use previous results from an all-sky search for isolated sources to constrain the continuous gravitational wave amplitude over a large and unexplored range of binary orbital parameters without explicitly performing a dedicated search for binary systems. The resulting limits are significantly more constraining than any existing upper limit for unknown binary systems, albeit the latter apply to different orbital parameter ranges.

Keywords: neutron stars — gravitational waves — continuous waves — binaries

1. INTRODUCTION

No search for continuous gravitational waves so far has produced clear evidence of a signal, including broadband and all-sky surveys (Abbott *et al* 2022, 2019; Steltner *et al* 2021; Dergachev & Papa 2022, 2021a,b, 2020).

The main signals targeted by these searches are fast rotating neutron stars with an equatorial deformation, an ellipticity $\varepsilon = (I_{xx} - I_{yy})/I_{zz}$, where I is the moment of inertia tensor and \hat{z} is aligned with the spin of the star. These searches are typically hierarchical, with a large number of candidates followed up through various stages of increasing sensitivity.

The most sensitive all-sky searches have targeted emissions from isolated objects. With many known millisecond pulsars in binary systems, it is reasonable to wonder whether a signal might have been dismissed as inconsistent with the assumed isolated model during the follow-up, because it in fact came from an object in a binary system.

This paper takes the first step in using results from a continuous wave isolated neutron star search, to investigate emissions from neutron stars with companions.

We identify orbital parameter ranges, for which a signal from a binary system would have appeared as a signal from an isolated object in the results of Stage 0 of Einstein@Home search (Steltner *et al* 2021). In this range, based on such results (Steltner *et al* 2021), we constrain the intrinsic gravitational wave amplitude from neutron stars in binary systems.

2. EXPLORING BINARY PARAMETER SPACE WITH ISOLATED CONTINUOUS WAVE SEARCHES

We perform a series of Monte-Carlo studies where continuous wave signals from sources in binary circular orbits are simulated in noiseless data. We consider an exhaustive range of projected orbital semi-major axis, orbital period and time of ascending nodes: $a_p \in [10^{-2}, 10^6]$ lightseconds, $P_b \in [10^{-6}, 10^5]$ years and $\psi_{asc} = 0, \pi/6, \pi/3, \pi/2$, with $\psi_{asc} = 2\pi t_{asc}/P_b$. Figure 1 shows the various orbital parameters and clarifies the symbols. The values of a_p and P_b are log-uniformly distributed. Each signal is searched for with the same semi-coherent $2\mathcal{F}$ search algorithm for isolated signals as used in Stage 0 (Steltner *et al* 2021), yielding a value of the SNR $\rho_{bin-iso}^2$, where the subscript means **binary** signal searched with an **isolated** signal model. The same

Corresponding author: Avneet Singh
avneet.singh@aei.mpg.de

Corresponding author: Maria Alessandra Papa
maria.alessandra.papa@aei.mpg.de

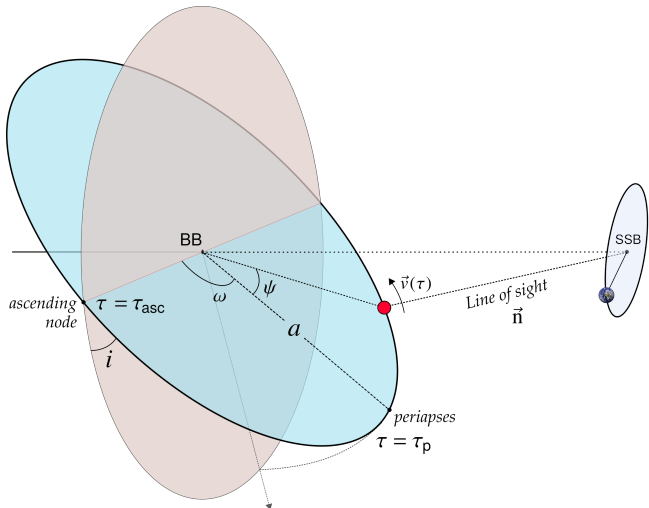


Figure 1. A nearly circular binary orbit. *Abbrev:* BB \equiv Binary Barycentre, SSB \equiv Solar System Barycentre. The projected semi-major axis is reported in units of time, lightseconds, i.e. $a_p = a \sin i / c$, and $P_b \sim 2\pi a / |\dot{v}|$ is the period of the binary orbit.

signal, but coming from an isolated object, is also simulated and searched for, and the $\rho_{\text{iso-iso}}^2$ is recorded. We define the SNR change \mathcal{L}_ρ for each search as

$$\mathcal{L}_\rho = \frac{\rho_{\text{iso-iso}}^2 - \rho_{\text{bin-iso}}^2}{\rho_{\text{max}}^2}, \quad (1)$$

where ρ_{max} is the maximum possible SNR, attainable for zero mismatch between signal and search template in all of the signal parameters. \mathcal{L}_ρ can be positive or negative; the negative values occur when loss of SNR due to a mismatch in phase parameters is compensated by the modulation due to the orbital parameters. For every signal, we also record the distance between the signal's phase parameters and the phase parameters recovered by the search. Figure 2 shows the distributions of \mathcal{L}_ρ .

We identify three regions in the $(a_p - P_b)$ plane : a) *indistinguishable* region where $\mathcal{L}_\rho < 1\%$ b) *distinguishable* region where $\mathcal{L}_\rho \leq 25\%$ c) the remaining region where $\mathcal{L}_\rho \sim 100\%$. In the indistinguishable region, the location of the maximum detection statistic in the parameter space due to a binary signal is statistically at the same distance from the signal parameters as the maximum from an isolated signal; in the distinguishable region however, this is not the case. These regions are shown in Figure 2 and they are broadly consistent with our predictions in (Singh *et al* 2019), albeit the case studied here is far more general and complete than that of (Singh *et al* 2019). The regions' boundaries are slightly different at the highest a_p values, depending on the value of ψ_{asc} . We have picked the boundaries in the most conservative way, i.e. so that the conditions on \mathcal{L}_ρ

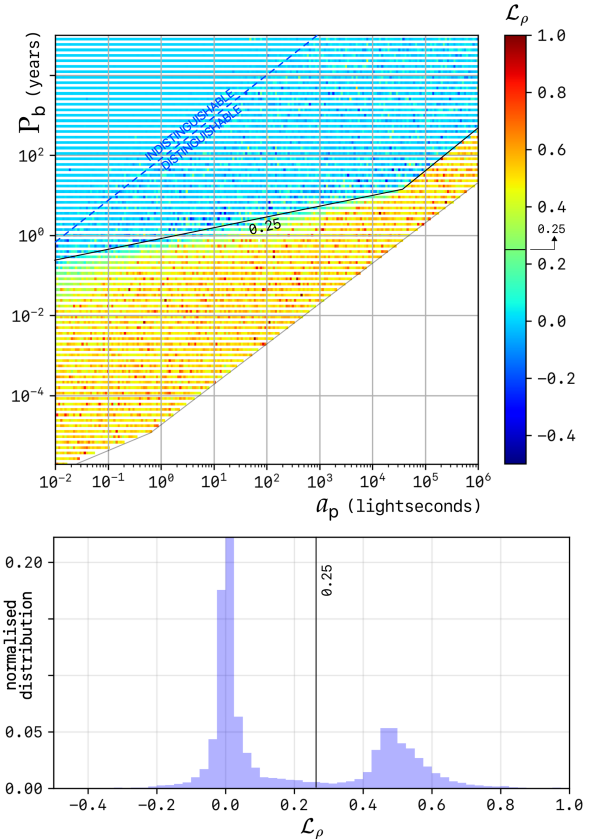


Figure 2. Distributions of \mathcal{L}_ρ of equation (1), based on 15,000 injections \mathcal{E} recoveries of simulated signals as described in the text with $\psi_{\text{asc}} = 0$ (for different values of ψ_{asc} the regions are very similar and, if anything, the yellow higher-loss region is slightly less extended).

above hold for any value of ψ_{asc} , and in particular for $\psi_{\text{asc}} = 0$.

Based on these findings, we use the results of Stage 0 of the Einstein@Home search for signals from isolated objects (Steltner *et al* 2021) to constrain the amplitude of continuous gravitational waves from neutron stars in binary systems in the distinguishable and indistinguishable regions in $a_p - P_b$ plane. We expect that the resulting upper limits will not be significantly less constraining than the limits set by Steltner *et al* (2021).

In practice, we take the most significant candidate from the Stage 0 results of Steltner *et al* (2021) in every 0.5 Hz band and find the value of the intrinsic gravitational wave amplitude $h_0^{90\%}$ such that 90% of the population of signals with binary parameters in distinguishable and indistinguishable regions would have produced a detection statistic equal to the observed value. This is the standard definition of the 90% confidence gravitational wave amplitude upper limit used in many continuous waves searches, including (Steltner *et al* 2021).

In order to determine $h_0^{90\%}$, we add fake signals to the real data and search for them with exactly the same procedure as used in the search (Steltner *et al* 2021), including data cleaning and candidate clustering. The resulting 90% constraints are shown in Figure 3. The sensitivity of the isolated searches to binary orbits degrades slightly with increasing frequency due to the linear dependence of the binary modulation on frequency. This is reflected in the slight worsening of constraints in our results (blue) above roughly 200 Hz in comparison to (Steltner *et al* 2021) (green).

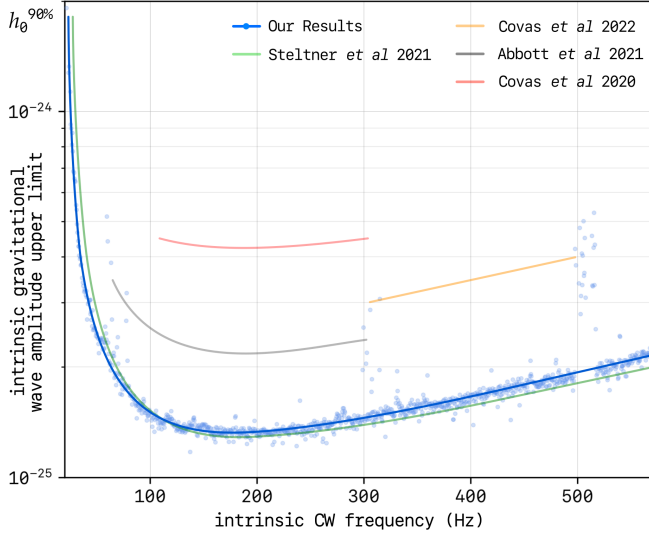


Figure 3. Constraints on the intrinsic amplitude of continuous gravitational waves ($h_0^{90\%}$) from neutron stars in binary orbits populating indistinguishable and distinguishable regions, as a function of the gravitational wave frequency (most likely twice the rotation frequency). To ease comparisons and guide the eye, we have plotted ‘smoothened’ results from previous searches for binary pulsars in LIGO data (Covas & Sintes 2020), (Covas *et al* 2022) and (Abbott *et al* 2021). Those searches cover a different part of binary parameter space, where dedicated and costly searches are necessary.

3. CONCLUSIONS

We have demonstrated that simply based on search results for signals from isolated objects, the gravitational wave amplitude of signals from neutron stars in long period binary systems (upper blueish region in Figure 2) can be constrained with remarkable sensitivity at practically zero cost.

The actual detection of such systems requires an additional search, but our results demonstrate that such search could be limited to following-up the candidates from the first stage of an isolated search. This allows to piggy-back on results obtained at a very large compu-

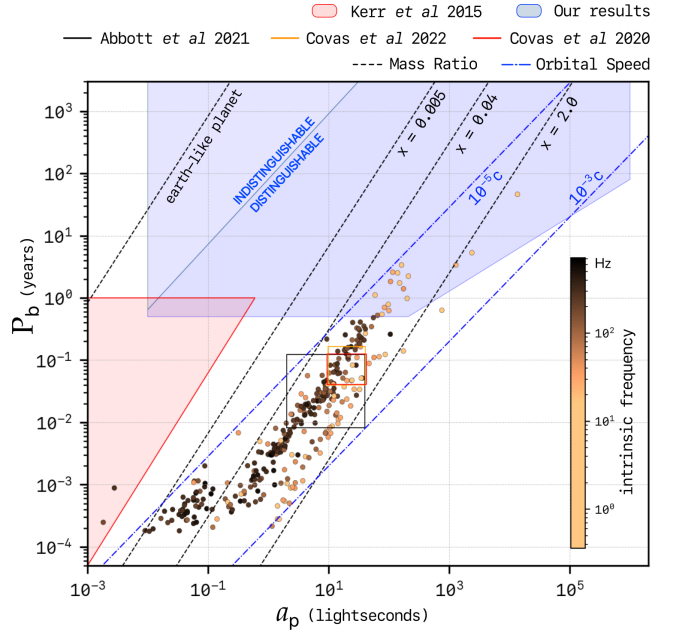


Figure 4. ATNF catalogue binary pulsars plotted in the $a_p - P_{\text{orb}}$ plane and color-coded by rotational frequency. The blue lines mark the contours of constant orbital speed, while the black lines demarcate contours of constant mass ratios ($x = M_c/1.4M_\odot$). The area where pulsar companions are deemed rare by Kerr *et al* (2015) is shaded in red; the areas constrained in this paper based on the results of Steltner *et al* (2021), are the “distinguishable” and “indistinguishable” areas above. The boxes mark the regions searched by previous gravitational wave searches.

tational cost and opens up a broad region of parameter space for investigation at sensitivities close to the highest levels achievable by continuous wave surveys from isolated objects.

In the ATNF pulsar catalogue there are no *binary* systems in a large part of the inspected binary parameter space, i.e. with periods longer than 30 days and lighter than $0.056M_\odot$ ($x < 0.04$). But four *3-body* systems are suspected/known to contain a pulsar, with a companion in this orbital parameter range: PSR B1620-26 (Ford *et al* 2000; Thorsett *et al* 1999), PSR B1257+12 (Wolszczan & Frail 1992), and perhaps PSR B0943+10 (Starovoit & Suleymanova 2019; Exoplanets 2014; Shaw *et al* 2022) and PSR J2007+3120 (Nitu *et al* 2022). The first two are millisecond pulsars, the last two spin at about 1 Hz, outside of the high sensitivity band of the current generation of gravitational wave detectors. The PSR B1620-26 is a pulsar-white-dwarf-planet system, with a $2.5M_{\text{Jup}}$ ($x = 0.0017$) mass planet in a 100 yr orbit around the two stars at a distance of about 10^4 lightseconds. The PSR B1257+12 system is composed of a pulsar and three planets, in orbits of 25, 67 & 98 day and 94, 180 & 230 lightseconds, respectively. The plan-

ets have masses $x = 4.3 \times 10^{-8}, 9.2 \times 10^{-6}, 8.4 \times 10^{-6}$, respectively.

The discussion above shows that, even if not commonly observed, pulsars with companions in the orbital parameter range that we have investigated, do exist.

Furthermore, since many new pulsars are monitored for relatively short periods of time, timing noise and the correlation of the orbital modulation with the intrinsic spin-down make it more likely that binary pairs with low-mass companions and/or long-periods may be misclassified as isolated, as for PSR J1024-0719 (Kaplan *et al* 2016). This has motivated dedicated searches for pulsars with companions (Antoniadis 2021; Nitu *et al* 2022), which however have not conclusively explored the entire parameter space that we consider here.

The observation of planetary pulsar systems can help shed light on important astrophysical processes in stel-

lar evolution and on stellar environments (see Kramer 2018, and references therein), and continuous gravitational waves might well add to the impressive armoury of high-precision pulsar timing in electromagnetic radio, gamma-ray and X-ray bands, as well as of optical observations.

4. ACKNOWLEDGMENTS

We are very grateful to Michael Kramer and John Antoniadis for insightful discussions. We thank Benjamin Steltner for his support in implementing the same pipeline as the Stage 0 of Steltner *et al* (2021), necessary for the upper limits of this search, and Bruce Allen for useful comments. The simulations for this study were performed on the ATLAS cluster at MPI for Gravitational Physics/Leibniz University Hannover.

REFERENCES

- Abbott B P *et al.* 2019, **Phys. Rev. D**, 100, 024004
 Abbott R *et al.* 2021, **Phys. Rev. D**, 103, 064017
 —. 2022, **arXiv**, 2201.00697, 23
 Antoniadis J. 2021, **MNRAS**, 501, 1116
 Covas P B, Papa M A, Prix R & Owen B J. 2022, **ApJ Lett.**, 929, 19
 Covas P B & Sintes A M. 2020, **Phys. Rev. Lett.**, 124, 191102
 Dergachev V & Papa M A. 2020, **Phys. Rev. Lett.**, 125, 171101
 —. 2021a, **Phys. Rev. D**, 103, 063019
 —. 2021b, **Phys. Rev. D**, 104, 043003
 —. 2022, **arXiv**, 2202.10598, 6
 Exoplanets Team. 2014, The Extrasolar Planets Encyclopaedia
 Ford E B, Joshi K J, Rasio F A & Zbarsky B. 2000, **ApJ**, 528, 336
 Kaplan D L *et al.* 2016, **ApJ**, 826, 86
 Kerr M, Johnston S, Hobbs G & Shannon R M. 2015, **ApJ Lett.**, 809, 11
 Kramer M. 2018, Pulsar Timing as an Exoplanet Discovery Method
 Nitu I C *et al.* 2022, **arXiv**, 2203.01136, 12
 Shaw B., Stappers B. W., Weltevrede P. *et al.* 2022, **Mon. Not. Roy. Astron. Soc.**, 513, 5861
 Singh A, Papa M A & Dergachev V. 2019, **Phys. Rev. D**, 100, 024058
 Starovoit E D & Suleymanova S A. 2019, **Astron. Rep.**, 63, 310
 Steltner B, Papa M A, Eggenstein H B *et al.* 2021, **ApJ**, 909, 79
 Thorsett S E, Arzoumanian Z, Camilo F & Lyne A G. 1999, **ApJ**, 523, 763
 Wolszczan A & Frail D A. 1992, **Nature**, 355, 145